Ratiometric dosing of anticancer drug combinations: Controlling drug ratios after systemic administration regulates therapeutic activity in tumor-bearing mice

Lawrence D. Mayer,[1] Troy O. Harasym,[1]
Paul G. Tardi,[1] Natashia L. Harasym,[1]
Clifford R. Shew,[1] Sharon A. Johnstone,[1]
Euan C. Ramsay,[2] Marcel B. Bally,[2]
and Andrew S. Janoff[1,3]

[1]Celator Pharmaceuticals Corp.; [2]Department of Advanced Therapeutics, BC Cancer Agency, Vancouver British Columbia, Canada; and [3]Celator Pharmaceuticals, Inc., Princeton, New Jersey

Abstract

Anticancer drug combinations can act synergistically or antagonistically against tumor cells *in vitro* depending on the ratios of the individual agents comprising the combination. The importance of drug ratios *in vivo*, however, has heretofore not been investigated, and combination chemotherapy treatment regimens continue to be developed based on the maximum tolerated dose of the individual agents. We systematically examined three different drug combinations representing a range of anticancer drug classes with distinct molecular mechanisms (irinotecan/floxuridine, cytarabine/daunorubicin, and cisplatin/daunorubicin) for drug ratio–dependent synergy. In each case, synergistic interactions were observed *in vitro* at certain drug/drug molar ratio ranges (1:1, 5:1, and 10:1, respectively), whereas other ratios were additive or antagonistic. We were able to maintain fixed drug ratios in plasma of mice for 24 hours after i.v. injection for all three combinations by controlling and overcoming the inherent dissimilar pharmacokinetics of individual drugs through encapsulation in liposomal carrier systems. The liposomes not only maintained drug ratios in the plasma after injection, but also delivered the formulated drug ratio directly to tumor tissue. *In vivo* maintenance of drug ratios shown to be synergistic *in vitro* provided increased efficacy in preclinical tumor models, whereas attenuated antitumor activity was observed when antagonistic drug ratios were maintained. Fixing synergistic drug ratios in pharmaceutical carriers provides an avenue by which anticancer drug combinations can be optimized prospectively for maximum therapeutic activity during preclinical development and differs from current practice in which dosing regimens are developed empirically in late-stage clinical trials based on tolerability. [Mol Cancer Ther 2006;5(7):1854–63]

Introduction

Combination chemotherapy regimens for cancer are typically developed by establishing the recommended dose of one agent and then adding subsequent drugs to the combination at increasing concentrations until the aggregate effects of toxicity are considered to be limiting (1–3). This approach assumes, perhaps incorrectly, that maximum therapeutic activity will be achieved with maximum dose intensity for all drugs in the combination and ignores the possibility that more subtle concentration-dependent drug interactions could result in frankly synergistic outcomes (4–6). Although a variety of approaches have been used to investigate whether drug combinations interact synergistically in cell culture systems (7–10), the use of such information to predict clinical activity has been questionable (11, 12).

One factor that clearly impedes the use of screening data to *a priori* predict synergy *in vivo* is the distinct pharmacology of different drugs used in combinations. In contrast to *in vitro* systems where drug concentrations exposed to tumor cells can be tightly controlled, individual agents in a conventional anticancer drug combination will distribute and be eliminated independently of each other after administration *in vivo*. This becomes important if the degree of synergy (or antagonism) depends, as it often does, on the concentration and ratio of the combined drugs (13–18). For example, when camptothecin and doxorubicin were exposed simultaneously to glioma cells at a molar ratio of 5:1, strong antagonism was observed, whereas a 1.5:1 ratio resulted in synergistic activity (18). Initial plasma drug/drug ratios will undoubtedly change within minutes after injection of conventional, aqueous-based drug combinations and such uncoordinated drug pharmacokinetics could lead to exposure of tumor cells to drug ratios with inferior therapeutic activity.

We describe herein the application of drug delivery technology to address this problem by controlling the release of drug combinations from the delivery vehicle such that fixed drug ratios are maintained after injection. Applying this "ratiometric" approach to combinations of common anticancer agents representing a range of drug

classes and target indications has enabled us to translate *in vitro* synergy information *in vivo*, resulting in fixed-ratio drug combination formulations with potent therapeutic activity.

Materials and Methods

Cell Culture

The human colorectal cell lines HCT-116, LS180, and HT-29; H460 non–small cell lung cancer line; and the Capan-1 pancreatic line were purchased from American Type Culture Collection (Manassas, VA). The murine Colon 26 carcinoma and P388 leukemia lines were obtained from the tumor repository at National Cancer Institute-Frederick. Cells were exposed to fixed ratios of drugs for 72 hours at eight concentrations along the profile of the most cytotoxic drug and viable cells were quantified using standard 3-(4,5-dimethylthiazol-2-yl)-2,5-diphenyltetrazolium bromide detection at 570 nm after DMSO addition (19).

Proliferation Data Analysis

Test data were converted to a percentage mean cell survival value relative to untreated control wells. The fraction of affected cells (f_a) was subsequently determined for each well. Three replicates were averaged and repeats of these data sets (minimum of three) were entered into CalcuSyn (Biosoft, Ferguson, MO) for analysis. This program uses the median effect analysis algorithm that produces the combination index (CI) value as a quantitative indicator of the degree of synergy or antagonism (20, 21). Using this analysis method, CI = 1.0 reflects additive activity, CI > 1 signifies antagonism, and a CI < 1.0 indicates synergy.

Drug Encapsulation

Irinotecan/Floxuridine. Distearoylphosphatidylcholine, distearoylphosphatidylglycerol, and cholesterol were dissolved at a molar ratio of 7:2:1 into dichloromethane/methanol/water (94:5:1), and the mixture was dried using nitrogen gas and then vacuumed overnight. The lipid film was hydrated to form multilamellar liposomes with 100 mmol/L copper gluconate/180 mmol/L TEA (pH 7.0) containing 25 mg/mL floxuridine and tracer quantities of [^{14}C]floxuridine for in-process analysis of encapsulated floxuridine. The hydrated films were extruded through 100 nm polycarbonate filters at 70°C and the mean diameter of the formulations used were 100 ± 20 nm as determined by quasi-elastic light scattering analysis (Submicron Particle Sizer Model 370, Nicomp Particle Systems, Santa Barbara, CA). Following extrusion, preparations were exchanged into 300 mmol/L sucrose/20 mmol/L HEPES/30 mmol/L EDTA (pH 7.0) by cross-flow filtration. Irinotecan was loaded by incubating the drug with the liposomes (0.12:1 molar ratio of irinotecan to lipid) at 50°C for 10 minutes to achieve a 1:1 molar encapsulated irinotecan/floxuridine ratio. Following drug loading, the liposome preparation was exchanged into saline with cross-flow filtration.

Daunorubicin/Cytarabine. Cytarabine containing liposomes were made in the same manner described above for floxuridine using a buffer pH of 7.4 and a cytarabine concentration of 50 mg/mL with a trace of [^{3}H]cytarabine for in-process analysis of cytarabine encapsulation. Following extrusion (22), the liposome preparation was exchanged into 20 mmol/L HEPES/150 mmol/L sodium chloride/1 mmol/L EDTA (pH 7.4) with cross-flow filtration. Daunorubicin loading was achieved by incubating the liposomes in the presence of the drug at 50°C for 30 minutes to achieve a 5:1 molar cytarabine/daunorubicin ratio.

Cisplatin/Daunorubicin. For liposomal cisplatin, dimyristoylphosphatidylcholine/cholesterol (55:45; mol/mol) lipid films were hydrated by vortexing in the presence of hot (80°C) 150 mmol/L NaCl solution containing cisplatin (28.3 mmol/L). The resulting suspension was extruded at 80°C. The preparations were cooled to room temperature, followed by centrifugation (1,250 × *g* for 5 minutes), to pellet any unencapsulated cisplatin. The external buffer was exchanged with 20 mmol/L HEPES, 150 mmol/L NaCl (HBS; pH 7.5) by dialysis. Encapsulated cisplatin concentrations were determined by diluting aliquots 1/10,000 in 0.1% nitric acid and analyzing via atomic absorption spectroscopy (Varian Model AA240Z). For liposomal daunorubicin, lipid films composed of distearoylphosphatidylcholine/2,000 MW polyethylene glycol–conjugated distearoylphosphatidylethanolamine at a 95:5 (mol/mol) ratio were hydrated with 300 mmol/L CuSO$_4$ solution at 70°C followed by extrusion at 70°C. The external buffer was exchanged using Sephadex G-50 columns equilibrated with HBS (pH 7.5). The resulting liposomes were loaded with daunorubicin by incubating for 10 minutes at 60°C at a drug-to-lipid ratio of 0.15:1 (mol/mol).

Pharmacokinetics

Samples were injected i.v. into female Rag2-M mice (Taconic, Germantown, NY) at the indicated doses. Following injection, mice (three per time point) were euthanized at various times and plasma isolated from EDTA-treated blood. For irinotecan analysis, 100 μL saline-diluted plasma samples were mixed with 600 μL acidified methanol and the supernatant was injected onto the high-performance liquid chromatography (HPLC). For floxuridine analysis, saline-diluted plasma samples were extracted in ethyl acetate (to which 5-chlorouracil was added as an internal standard), dried, and reconstituted in water (pH 2). For daunorubicin analysis, 10 μL plasma samples were mixed with 490 μL acidified methanol, centrifuged at 1,500 rpm for 10 minutes, and the supernatant was injected onto the HPLC. For cytarabine analysis, 10 μL plasma samples were mixed with 50 μL methanol by vortexing and were added to 440 μL water. Plasma aliquots of mice receiving liposomal cisplatin were processed as described above for platinum detection using atomic absorption spectrometry (Varian Model AA240Z).

HPLC Drug Analysis

Irinotecan was quantified using a Waters Symmetry C18 column with a multi–λ fluorescence detector (Waters Model 2475) set at excitation/emission wavelengths of 362/425 nm. The mobile phase was 1.5 mL/min acetonitrile–75 mmol/L ammonium acetate containing 7.5 mmol/L tetrabutylammonium bromide (24:76, v/v; pH 6.4). Floxuridine was quantified using a Waters Xterra MS C18

column and a photodiode array detector set at a wavelength of 266 nm. The mobile phase was 100% HPLC grade water adjusted to pH 2.0 using perchloric acid. Cytarabine was evaluated using a Phenomenex Luna C18(2) reverse phase analytic column with photodiode array detector (λ = 273.7 nm). The mobile phase was 1 mL/min 25 mmol/L ammonium acetate (pH 4.8). Daunorubicin was evaluated using a Phenomenex Luna C18(2) reverse phase analytic column with a multi$-\lambda$ fluorescence detector set at excitation/emission wavelengths of 480/560 nm. The mobile phase was 1 mL/min 25 mmol/L ammonium acetate (pH 4.8)/acetonitrile (67.5:32.5, v/v).

Efficacy Evaluations

For the HT-29, Capan-1, and H460 tumor cells, 2×10^6 cells were inoculated s.c and 1×10^6 cells for the Colon 26 model. Tumor weights were determined according to the equation (length $\times$ width^2) / 2 using direct caliper measurements (23, 24). Maximum tolerated dose (MTD) values were defined as survival in the absence of significant tumor burden with $\leq$15% body weight loss nadir lasting $\leq$2 days. For P388 studies, mice were inoculated i.p. on day 0 with 1×10^6 cells. Ascitic tumor progression, survival, and body weight were monitored daily. Moribund mice were euthanized and the time of death was logged as the following day. Efficacy experiments were generally repeated to confirm the observed comparative trends. Tumor log cell kill values were determined for individual mice and the statistical significance between different treatment groups was determined using the *post hoc* Student-Newman-Keuls analysis method subsequent to one-way ANOVA (25–27).

Results

We evaluated the *in vitro* cytotoxicity of various anticancer drug combinations using the median-effect analysis method of Chou et al. (20, 28, 29), where the measure of synergy is defined by the CI value. The selection of this drug interaction analysis method was based on its suitability for assessing whether drugs interact synergistically (CI < 1.0), additively (CI $\sim$ 1.0), or antagonistically (CI > 1.0) as a function of drug concentration for different fixed drug/drug ratios. Figure 1A and B summarizes the results of a synergy analysis done by exposing human colorectal and pancreatic cancer cells to various ratios and concentrations of irinotecan and floxuridine. Irinotecan and fluorinated pyrimidine are currently the standard of care in metastatic colorectal cancer, and the combination of irinotecan and the floxuridine-related 5-fluorouracil has been shown previously to interact synergistically *in vitro* under appropriate conditions (30–32). It should be noted that we chose to focus our *in vitro* evaluations on irinotecan rather than its more potent metabolite SN-38, because this reflects the situation experienced for liposomal delivery of irinotecan *in vivo* where preferential extravasation and accumulation of liposomes in tumors provide a local infusion reservoir of irinotecan (see below). Also, in contrast to irinotecan, SN-38 is extremely membrane permeable and was not amenable to stable retention in liposomal delivery systems after injection.
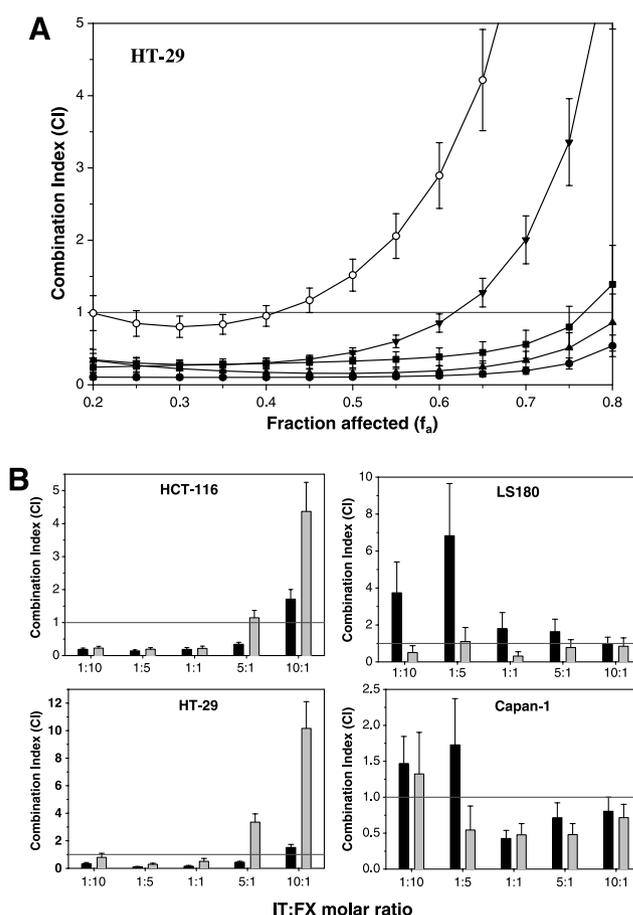

Figure 1. **A,** *in vitro* screening of irinotecan and floxuridine for synergy in HT-29 colorectal cells as a function of irinotecan/floxuridine ratio and drug concentration. Concentrations of fixed irinotecan/floxuridine molar ratios were titrated to provide a broad range of cell growth inhibition (reflected by f_a). *Points,* average values from triplicate assays repeated a minimum of thrice, where CI values of <1, $\sim$ 1, and >1 indicate synergy, additivity, and antagonism, respectively. Irinotecan/floxuridine molar ratios were 1:10 (■), 1:5 (●), 1:1 (▲), 5:1 (▼), and 10:1 (○). *Bars,* SE determined for the indicated f_a values. **B,** *in vitro* screening CI results from various cell types plotted at ED$_{50}$ (*black columns,* f_a = 0.5) and ED$_{75}$ (*gray columns,* f_a = 0.75) as a function of irinotecan/floxuridine (*IT:FX*) ratio.

For HT-29 cells, evidence of significant variation of CI as a function of drug ratio was observed (Fig. 1A and B), particularly at high drug concentrations (high f_a). Strong antagonism reflected by CI values >4 was seen at irinotecan/floxuridine molar ratios of 5:1 and 10:1, whereas synergy was evident at ratios of 1:1, 1:5, and 1:10 (CI values <0.5). At drug concentrations giving rise to 50% and 75% tumor growth inhibition (ED$_{50}$ and ED$_{75}$, corresponding to f_a = 0.50 and 0.75, respectively), a similar trend of ratio-dependent synergy was observed for HCT-116 human colorectal cancer cells (Fig. 1B), where CI values <0.5 were obtained at irinotecan/floxuridine ratios of 1:1, 1:5, and 1:10, and strong antagonism (ED$_{75}$ CI = 4.4) was seen at an irinotecan/floxuridine ratio of 10:1. Ratio-dependent CI profiles observed for LS180 human colorectal cancer and

Capan-1 human pancreatic tumor lines were different in that antagonism was observed at low irinotecan/floxuridine ratios (1:10 and 1:5); however, the irinotecan/floxuridine molar ratio of 1:1 consistently provided synergy across all four gastrointestinal cell lines and avoided antagonism (Fig. 1B). The degree of drug ratio dependency was greatest in gastrointestinal tumor lines; however, expanded analysis of ratio-dependent synergy in additional tumor cell lines confirmed that the 1:1 irinotecan/floxuridine ratio was optimal (data not shown). We surmised that if similar relationships between drug/drug ratio and antitumor activity were to hold *in vivo*, we would be able to achieve significant increases in efficacy by controlling individual drug pharmacokinetics and maintaining the optimal 1:1 ratio after systemic administration. It should also be noted that ratio-dependent synergy was observed for combinations of floxuridine with SN-38; however, optimal activity occurred at much lower SN-38/floxuridine molar ratios. Specifically, at ED_{75}, in HT-29 cells, CI values >1.0 were observed for SN-38/floxuridine molar ratios of 1:1, 1:10, and 1:100, whereas CI values <1.0 were obtained at a SN-38/floxuridine ratio of 1:1,000 (data not shown).

We coencapsulated irinotecan and floxuridine at a 1:1 molar ratio inside 100-nm-diameter liposomes composed of distearoylphosphatidylcholine/distearoylphosphatidylglycerol/cholesterol (7:2:1 molar ratio) at a 0.1:1 drug-to-lipid ratio (mol/mol). Floxuridine was passively encapsulated during liposome formation and unentrapped floxuridine was subsequently removed via dialysis. Irinotecan was entrapped using a copper-based active loading procedure whereby the drug accumulates inside preformed liposomes containing copper gluconate/TEA (pH 7.0; ref. 33). This formulation (hereafter called CPX-1) maintained the irinotecan/floxuridine molar ratio near 1:1 over extended times (up to 24 hours) after i.v. injection into mice (Fig. 2). In
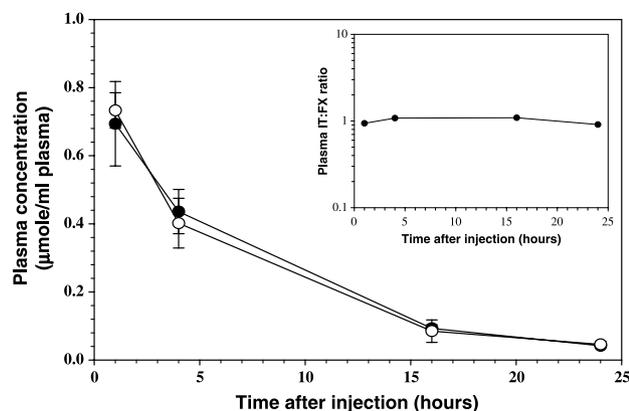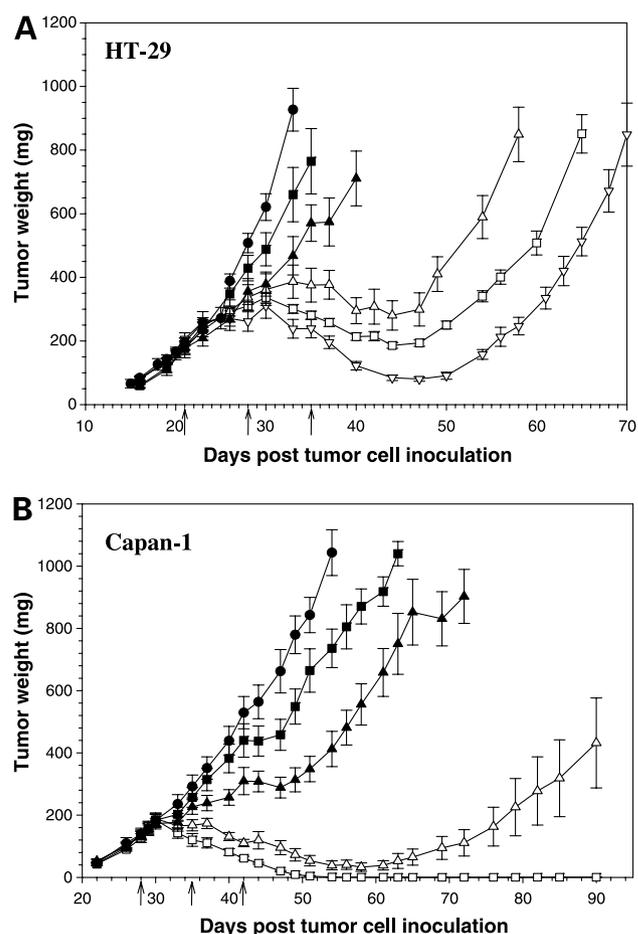

Figure 3. Efficacy of irinotecan and floxuridine codelivered in CPX-1 against gastrointestinal solid tumor models. HT-29 and Capan-1 tumor-bearing Rag2-M mice (six per group) were treated i.v. on the days indicated by the arrows. *Bars,* SE. Doses are expressed in μmol/kg. **A,** irinotecan/floxuridine efficacy in the HT-29 CRC model. ●, saline; ■, irinotecan/floxuridine in saline (37:37); ▲, irinotecan/floxuridine in saline (148:148); △, CPX-1 (irinotecan/floxuridine, 18.5:18.5); □, CPX-1 (irinotecan/floxuridine, 37:37); ▽, CPX-1 (irinotecan/floxuridine, 74:74). **B,** irinotecan/floxuridine efficacy in the Capan-1 pancreatic model. ●, saline; ■, irinotecan/floxuridine in saline (37:37); ▲, irinotecan/floxuridine in saline (148:148); △, CPX-1 (irinotecan/floxuridine, 18.5:18.5): □, CPX-1 (irinotecan/floxuridine, 37:37).

Figure 2. Plasma drug concentrations for irinotecan (●) and floxuridine (○) upon i.v. administration of CPX-1 (37:37 μmol/kg) to Rag2-M female mice (*n* = 3 per time point). *Bars,* SD. Plasma was extracted and analyzed by HPLC as described in Materials and Methods. *Inset,* circulating plasma irinotecan/floxuridine (IT:FX) molar ratio calculated from the absolute plasma concentrations.

addition, the plasma area under the curve (AUC_{0-last}) values for irinotecan and floxuridine administered as CPX-1 were ∼1,500 and 750 times greater, respectively, than observed for the same dose of drugs coadministered in saline (data not shown). HPLC analysis showed that the circulating liposomal drug formulations contained intact drug; no evidence of degradation was observed for either agent. Circulating plasma drug-to-lipid ratios decreased over time with a half-life of ∼7.5 hours for both drugs, indicating that irinotecan and floxuridine were released systemically from the liposomes at a 1:1 molar ratio. However, SN-38 was not detected using the HPLC quantification method here for plasma samples obtained from mice.

Table 1. Quantitative analysis of CPX-1 *in vivo* antitumor activity in human HT-29 colorectal cancer and Capan-1 pancreatic xenograft tumor models

	Treatment groups							
	Column A	Column B	Column C	Column D	Column E	Column F	Column G	Column H
	CPX-1 (liposomal IT/FX at a 1:1 ratio)	IT in saline	FX in saline	IT/FX in saline at a 1:1 ratio	IT/FX in saline at a IT_{MTD}/FX_{MTD} ratio	Lipo-IT	Lipo-FX	Liposomal IT/FX at the antagonistic ratio
						Low dose / High dose	Low dose / High dose	
HT-29 colorectal								
Log cell kill value	1.71*	0.09	0.09	0.23	0.57	ND / 1.51	ND / 0.14	1.48
Dose (µmol/kg)	74:74[†]	148[†]	1,000[†]	148:148[†]	148:1,000[†]	ND / 74[†]	ND / 74[†]	74:7.4[†]
Capan-1 pancreatic								
Log cell kill value	1.81*	0.65	0.43	0.69	ND	1.15 / 1.46	0.30 / 0.43	0.56
Dose (µmol/kg)	37:37	148[†]	1,000[†]	148:148[†]	ND	7.4 / 37	37 / 74[†]	7.4:74[†]

NOTE: Log cell kill = $[T - C] / [(3.32) (T_d)]$, where $T - C$ is the treatment-induced delay for tumors to reach 400 to 500 mg, and T_d is the tumor doubling time (7 days for both tumor models).
Abbreviations: IT, irinotecan; FX, floxuridine; ND, not determined.
*Statistically different ($P < 0.05$) from all other groups using Student-Newman-Keuls analysis.
[†]Indicates MTD.

Treatment of established HT-29 tumors with the fixed ratio formulation of irinotecan/floxuridine, CPX-1, yielded dose-dependent therapeutic activity with tumor regression at irinotecan/floxuridine doses of ≥18.5:18.5 µmol/kg (Fig. 3A). This activity was significantly greater than observed with irinotecan and floxuridine coadministered in saline at a 1:1 molar ratio escalated to its MTD of 148:148 µmol/kg (equivalent to a mg/kg-based irinotecan/floxuridine dose of 100:37). Similar results were seen in the Capan-1 tumor model, where CPX-1 at a dose of 37:37 µmol/kg resulted in complete tumor regressions that extended beyond day 90, whereas treatment with a 4-fold greater dose of the combination in saline at its MTD (148:148 µmol/kg) provided only modest tumor growth inhibition (Fig. 3B). Reducing the dose of CPX-1 to 18.5:18.5 µmol/kg lead to prolonged tumor regression and although no long-term complete responses were observed, the antitumor activity in this group was significantly greater than the 8-fold higher dose of the saline-based drug combination. The weekly dosing schedule used here for the human xenograft models was selected based on previous studies demonstrating the superior activity of this schedule for floxuridine as well as the current clinical dosing regimen used for irinotecan/5-fluorouracil combination chemotherapy (34).

We calculated tumor cell kill values from treatment-related delays in tumor growth using well-established analysis methods to compare treatment groups in a more quantitative fashion (Table 1; see ref. 35). Against HT-29 tumors, CPX-1 exhibited a maximum log cell kill value of 1.71 (Table 1, column A), reflecting antitumor activity that was 42 times greater than the MTD of either drug dosed individually in saline [log cell kill value of 0.09 for both 1,000 µmol/kg irinotecan (column B) and 148 µmol/kg floxuridine (column C); Table 1] and 30 times greater than the MTD of the two drugs coadministered in saline at a 1:1 molar ratio (log cell kill value of 0.23 for 148:148 µmol/kg irinotecan/floxuridine; Table 1, column D). In addition, CPX-1 was 14 times more active than a saline-based combination in which each drug was escalated to its MTD (log cell kill value of 0.57 for 148:1,000 µmol/kg irinotecan/floxuridine; Table 1, column E). When compared with liposomal formulations of the individual drugs, CPX-1 was ~1.6 times more active than irinotecan encapsulated in liposomes [log cell kill value of 1.51 for 74 µmol/kg liposome-encapsulated (lipo-) irinotecan; Table 1, column F] despite the fact that lipo-floxuridine was minimally active against this tumor model. In addition, CPX-1 was 1.7 times more active than 74:7.4 µmol/kg irinotecan/floxuridine coencapsulated inside liposomes at the *in vitro* antagonistic ratio of 10:1.

In the more floxuridine-sensitive Capan-1 tumor model, we were able to coencapsulate and dose therapeutically active amounts of both drugs at synergistic and antagonist irinotecan/floxuridine ratios identified *in vitro* (1:1 and 1:10, respectively; see Capan-1 panel of Fig. 1B). Here, it was clear that floxuridine inhibited irinotecan activity at the antagonistic ratio (see Table 1). Specifically, a log cell kill value of 0.56 was obtained for the liposome-formulated antagonistic ratio dosed at 7.4 µmol/kg irinotecan plus 74 µmol/kg floxuridine (Table 1, column H). Surprisingly, the matched dose of liposome encapsulated irinotecan alone (7.4 µmol/kg; Table 1, column F) provided an elevated log cell kill value of 1.15, which was significantly greater than observed for the same dose of irinotecan to which floxuridine was combined in the liposomes at an antagonistic ratio. In contrast, irinotecan and floxuridine coformulated as CPX-1, at the *in vitro* identified synergistic 1:1 molar ratio (37:37 µmol/kg), led to increased antitumor activity, where the log cell kill

Table 2. Quantitative comparison of CPX-1 *in vivo* antitumor activity in the murine Colon 26 colon carcinoma model (treatment days 9, 13, and 17)

Treatment	Dose (µmol/kg)	$T - C$ (d)	Log cell kill
Lipo-FX	30	2.9 ± 0.9	0.7
Lipo-IT	30	2.7 ± 0.3	0.6
CPX-1	30:30	10.4 ± 0.9	2.5*

NOTE: Log cell kill = $[T - C \,/\, (3.32)(T_d)]$, where $T - C$ is the treatment-induced delay for tumors to reach 500 mg (+SD, $n = 6$) and T_d is the tumor doubling time.

*Statistically different ($P < 0.001$) from all other groups using Student-Newman-Keuls analysis.

value of 1.81 for CPX-1 (column A) was greater than the value of 1.46 for the matched dose of 37 µmol/kg liposome-entrapped irinotecan (column F). Thus, we were able to conclude that whether irinotecan and floxuridine delivered in liposomes acted synergistically or antagonistically *in vivo* depended on the ratio of the two agents and was not due solely to the altered pharmacokinetics produced by the delivery vehicle. This was corroborated by efficacy results in the yet more floxuridine-sensitive Colon 26 murine colorectal cancer model (Table 2), where CPX-1 treatment yielded a log cell kill value of 2.5, which reflected ∼60 times more antitumor activity than the individual liposomal drugs and 10 times greater antitumor activity than predicted for additivity. Specifically, the log cell kill values of lipo-floxuridine (0.7) and lipo-irinotecan (0.6) at the same doses used in CPX-1 predict a log cell kill value of 1.3 for additivity, which is significantly less than the observed value of 2.5 for CPX-1 (Table 2). It is important to note that the ability of distearoylphosphatidylcholine/distearoylphosphatidylglycerol/cholesterol liposomes to maintain fixed drug ratios for extended times after i.v. injection was not dependent on the initially formulated drug ratio between irinotecan/floxuridine molar ratios of 10:1 to 1:10 (data not shown).

To establish whether circulating irinotecan/floxuridine ratios reflected those exposed to tumor tissue, CPX-1 liposomes containing coencapsulated [3H]irinotecan and [14C]floxuridine were administered to mice bearing established Capan-1 solid tumors and tumor-associated drug levels were determined by scintillation counting of tissue homogenates (correcting for tumor blood volume drug contributions). As shown in Fig. 4A, both drugs accumulated in Capan-1 tumors at similar rates with peak tumor concentrations of ∼15 nmol/g tumor at 4 hours, which remained associated with the tumor for extended times. As shown in Fig. 4B, these concentrations reflected tumor-associated irinotecan/floxuridine molar ratios near 1:1 through 8 hours after injection, which subsequently increased to 3:1 by 24 hours, all of which were within the synergistic irinotecan/floxuridine ratio range determined *in vitro* (compare Figs. 4B and 1B). It should be noted that tumor-associated irinotecan and floxuridine levels determined here reflect a compilation of drugs both inside and outside of the liposomes as well as radionuclide-bearing

metabolites. A more detailed comparison of these data with results from *in vitro* experiments will require separation of intracellular and extracellular drug pools and quantification of active drug metabolites.

We also found a fixed ratio of cytarabine and daunorubicin to be strongly synergistic *in vivo*. These drugs are currently used to treat acute myeloid leukemia and when screened against P388 leukemia cells *in vitro*, we found the combination capable of producing increasing synergy with increasing concentration (Fig. 5A). At drug concentrations providing 90% cell kill (ED$_{90}$, equivalent to a $f_a = 0.9$), cytarabine/daunorubicin molar ratios of 1:1, 5:1, and 10:1 exhibited synergistic CI values of 0.65, 0.72, and 0.75, respectively, whereas ratios of 1:5 and 1:10 displayed antagonistic CI values of ∼1.5 and 1.2, respectively (Fig. 5B).
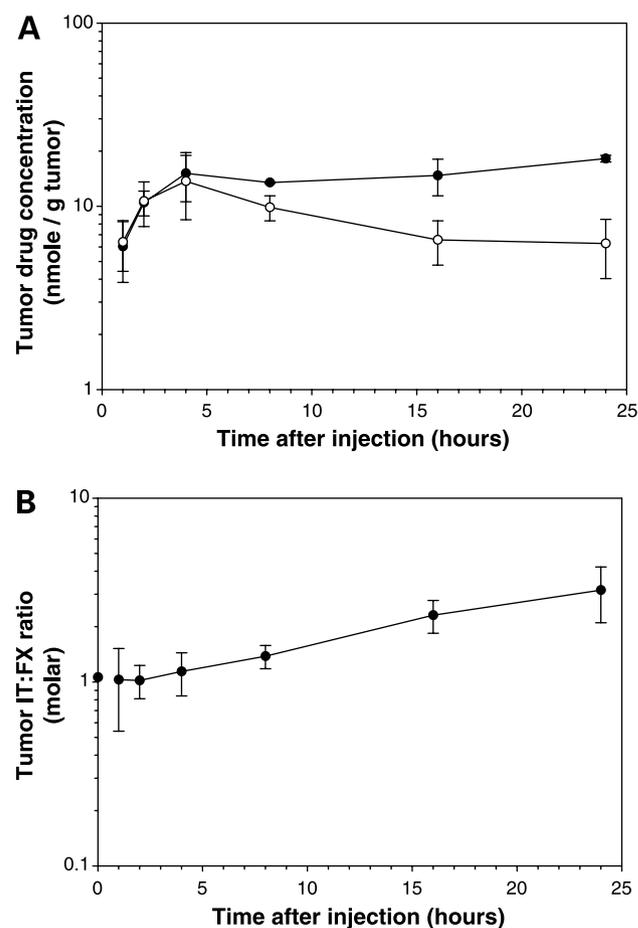
Figure 4. **A,** tumor accumulation of irinotecan (●) and floxuridine (○) after i.v. injection of [3H]irinotecan and [14C]floxuridine containing CPX-1 at an irinotecan/floxuridine dose of 37:37 µmol/kg to Rag2-M mice bearing s.c. Capan-1 tumors. Tumor homogenates were digested, quantified for 3H and 14C by scintillation counting, and tumor drug concentrations were determined after correcting for drug levels contributed by tumor-associated plasma volumes. *Points,* mean of three repeats; *bars,* SD. **B,** corresponding Capan-1 tumor-associated irinotecan/floxuridine (IT:FX) ratios over 24 h after injection of CPX-1.
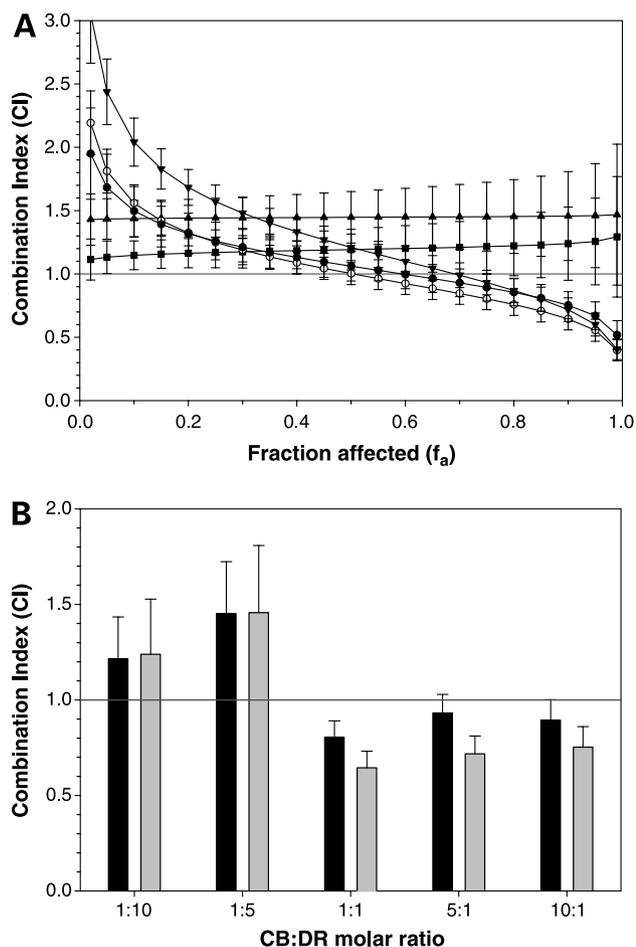
Figure 5. *In vitro* screening of cytarabine and daunorubicin for synergy in murine P388 leukemia cells. **A,** CI values presented as a function of cytarabine/daunorubicin ratio and f_a values. Conditions for assessing *in vitro* synergy were the same as described in Fig. 1. Cytarabine/daunorubicin molar ratios were as follows: 1:10 (■), 1:5 (▲), 1:1 (○), 5:1 (▼), and 10:1 (●). *Bars,* SE determined for the indicated f_a values. **B,** *in vitro* CI values at ED$_{75}$ (*black columns,* $f_a = 0.75$) and ED$_{90}$ (*gray columns,* $f_a = 0.90$) as a function of cytarabine/daunorubicin (*CB:DR*) ratio.

We developed a liposome formulation fixing cytarabine/daunorubicin at a ratio of 5:1 (hereafter called CPX-351) using the same lipid composition and encapsulation techniques established for CPX-1. CPX-351 maintained circulating cytarabine/daunorubicin molar ratios near 5:1 over 24 hours after i.v. administration (Fig. 6A, *inset*). Plasma drug elimination half-lives for both cytarabine and daunorubicin were ~12 hours, which reflected removal of intact, drug-containing liposomes from the circulation as well as release of the drugs from liposomes in the central blood compartment (release half-life of ~16 hours, data not shown). The latter variable was determined by monitoring the decrease in plasma drug to liposomal lipid ratio over time (determination of drug content by HPLC and liposomal lipid content using [^{14}C]dipalmitoylphosphatidylcholine as a lipid tracer). This formulation adminis-

tered at a dose of 50:10 μmol/kg cytarabine/daunorubicin (equivalent to a mg/kg-based cytarabine/daunorubicin dose of 12:5.3) achieved a 90% cure rate against P388 tumors *in vivo*, which was superior to the activity of cytarabine and daunorubicin administered as a combination in saline at their respective MTDs (2,500:20 μmol/kg cytarabine/daunorubicin), as well as the matched doses of the individual liposomal drugs (10 μmol/kg lipo-daunorubicin, 50 μmol/kg lipo-cytarabine; see Fig. 6B). Furthermore, the therapeutic activity of CPX-351 administered on a day 1, 4, 7 schedule (90% long-term survival) was superior to a free drug schedule where cytarabine was administered i.v. daily on days 1 to 5 at its MTD of 200 mg/kg per injection (17-day median survival time reflecting an increase in life span of 112%; data not shown).

To address the question of *in vivo* synergy directly, we turned to quantitative analysis and worked at
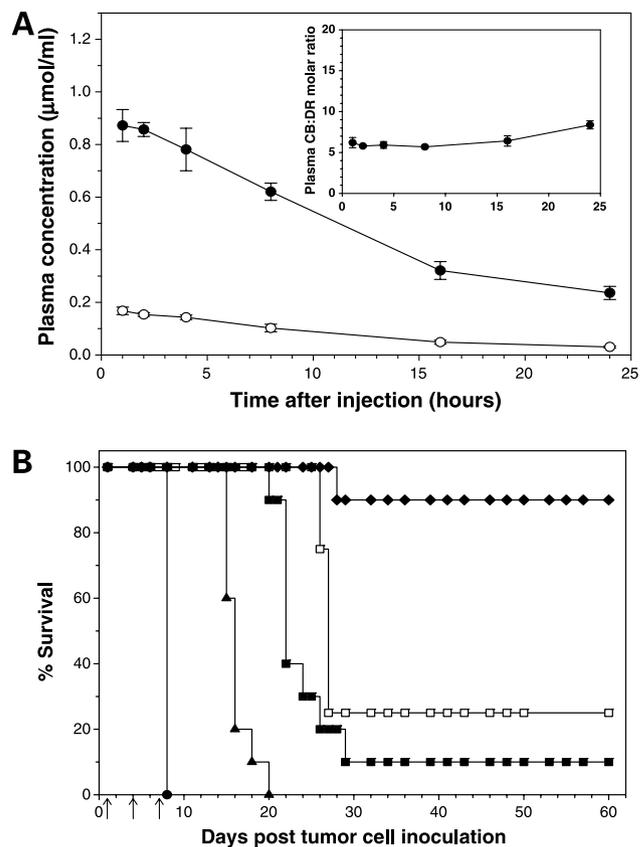

Figure 6. *In vivo* activity of cytarabine/daunorubicin encapsulated inside liposomes at a 5:1 molar ratio. **A,** plasma drug concentrations for cytarabine (●) and daunorubicin (○) determined by HPLC after i.v. administration of CPX-351 at 50:10 μmol/kg cytarabine/daunorubicin to BDF$_1$ female mice (n = 3 per time point). *Points,* mean; *bars,* SD. *Inset,* cytarabine/daunorubicin (CB:DR) ratio in plasma over 24 h. **B,** antitumor activity in the murine P388 ascites lymphocytic leukemia model. The following treatments were administered i.v. after i.p. inoculation of tumor cells (6–10 mice per group): ●, saline; ▲, lipo-daunorubicin (10 μmol/kg); □, cytarabine/daunorubicin in saline (2,500:20 μmol/kg); ■, lipo-cytarabine (50 μmol/kg); ♦, CPX-351 (cytarabine/daunorubicin, 50:10 μmol/kg). *Arrows,* treatment days.

Table 3. Quantitative comparison of CPX-351 *in vivo* antitumor activity in the murine P388 leukemia model

Treatment	Dose (µmol/kg)	MST (d)	Net MST (d)	Log cell kill
Saline	—	8.0	—	—
Lipo-CB	20	16.0	8.0	3.6
Lipo-DR	4	12.0	4.0	1.8
CPX-351	20:4	27.5	19.5	8.8

NOTE: Log cell kill = $[T - C / (3.32)(T_d)]$, where $T - C$ is the net median survival time of the treatment group compared to control and T_d is the tumor doubling time (0.67 days).
Abbreviations: CB, cytarabine; DR, daunorubicin; MST, median survival time.

intermediate doses to allow comparisons with individual liposomal drugs. CPX-351 dosed at ~50% of its MTD (20:4 µmol/kg cytarabine/daunorubicin) resulted in a net median survival time (median survival time$_{treatment}$ − median survival time$_{control}$) of 19.5 days, reflecting a log cell kill of 8.8 (Table 3). This activity was >2,000 times greater than what would be expected if each encapsulated drug had contributed in only an additive fashion to its activity. Specifically, log cell kill values of 3.6 for 20 µmol/kg lipo-cytarabine and 1.8 for 4 µmol/kg lipo-daunorubicin predict a log cell kill value of 5.4 for CPX-351 (see Table 3), which was significantly lower than the observed log cell kill value of 8.8. In addition, decreasing the cytarabine/daunorubicin ratio <5:1 lead to decreased antitumor activity in the P388 tumor model (data not shown).

To further test the concept that we could capture synergistic anticancer drug interactions determined through *in vitro* screening by maintaining fixed drug ratios *in vivo*, we identified a combination in which the antagonistic ratio could be administered at a higher dose than the synergistic ratio. When exposed to H460 cells in culture, cisplatin and daunorubicin interacted synergistically at a 10:1 molar ratio (CI = 0.75 at ED$_{80}$) and antagonistically at a 1:1 molar ratio (CI = 1.6 at ED$_{80}$). Encapsulating cisplatin and daunorubicin in separate liposomes enabled us to avoid interactions between daunorubicin and the chemically reactive cisplatin. We encapsulated cisplatin inside 100 nm dimyristoylphosphatidylcholine/cholesterol (55:45 molar ratio) liposomes and daunorubicin in distearoylphosphatidylcholine/2,000 MW polyethylene glycol–conjugated distearoylphosphatidylethanolamine liposomes, and mixed the two liposomal drug preparations at a 10:1 ratio to provide a putatively synergistic formulation and at a 1:1 ratio to provide a putatively antagonistic formulation. Figure 7A shows that each ratio was sustained in plasma over time after i.v. injection in mice. When both formulations were administered to H460 tumor-bearing mice at equivalent doses of cisplatin, the 1:1 antagonistic formulation was less active although it contained 10 times more daunorubicin than the drugs formulated at the 10:1 molar ratio (7.0 versus 0.7 µmol/kg, respectively; see Fig. 7B).

Discussion

Anticancer drug combinations continue to be developed in the clinic by escalating the individual agents to MTD (36). Although intuitive, this approach does not take into account the fact that many agents exert multiple pharmacologic effects with distinct concentration/activity relationships and that many of the molecular pathways associated with these effects have the potential to interact. This opens the possibility that the way in which drug combinations exert their antitumor effects may depend on the ratio of the drugs being combined. We focused our efforts on elucidating whether the ratio of drugs in a combination could dictate antitumor activity *in vitro* and *in vivo*. Although
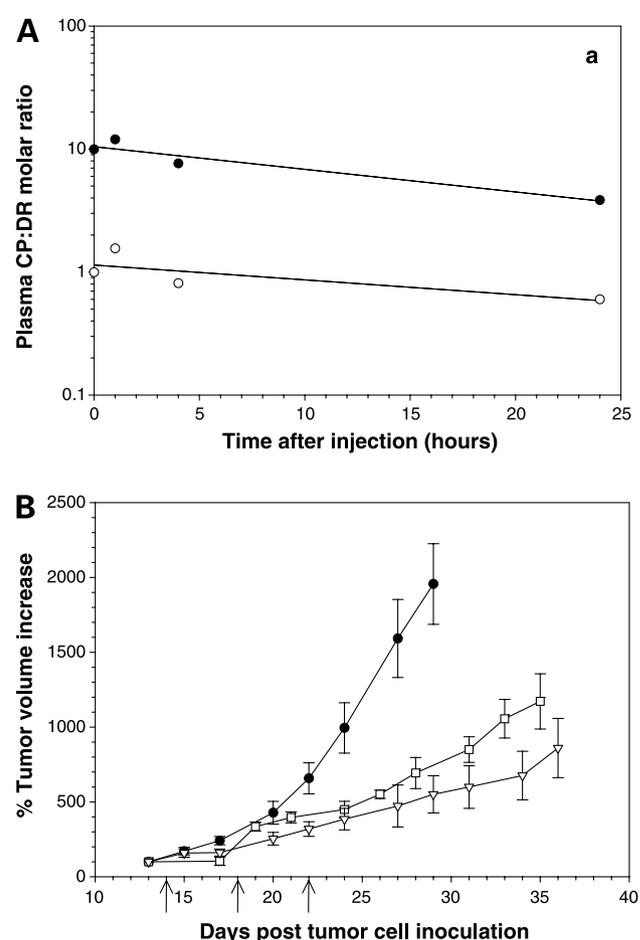
Figure 7. **A,** plasma drug molar ratios over 24 h for cisplatin (*CP*; determined by atomic absorption) and daunorubicin (*DR*; determined by HPLC) upon i.v. administration of 10:1 (●) and 1:1 (○) molar ratios of lipo-cisplatin and lipo-daunorubicin to female Rag2-M mice. **B,** *in vivo* evaluation of antitumor activity for 10:1 and 1:1 molar ratios of lipo-cisplatin/lipo-daunorubicin in the H460 human lung cancer xenograft model. Increases in percent tumor volume from day 13 after tumor inoculation were monitored for each group. *Points,* mean; *bars,* SE. Intravenous treatments were administered to mice (8–10 mice per group) on days 14, 18, and 22 after s.c. inoculation of tumor cells (*arrows,* treatment days). Treatment groups were as follows: ●, saline; □, lipocisplatin + lipo-daunorubicin (7:7; µmol/kg); ▽, lipo-cisplatin + lipo-daunorubicin (7:0.7; µmol/kg).

such an analysis has not been previously undertaken, the concept that maximum therapeutic activity of drug combinations may occur at doses below the MTD of one or more of the agents is not unprecedented. For example, low-dose suramin combined with paclitaxel has exhibited signs of promising antitumor activity both preclinically and clinically, while avoiding the significant toxicities experienced with suramin administered at MTD (4, 13). Also, optimal activity of certain biological response modifiers and signal transduction inhibitors has been observed at sub-MTD doses (37, 38). In a related treatment approach, ''metronomic'' dosing, where drugs are administered frequently at doses significantly below their MTD, has led to improved efficacy compared with less frequent dosing at MTD (5, 16). Although this approach uses low-dose administration of cytotoxic agents to induce antitumor effects indirectly through their action on endothelial cells rather than directly on the tumor cells themselves, it highlights the fact that pharmacologic targets can change as the drug dose is altered.

Despite the evidence cited above, drug combinations have not been systematically evaluated for ratio-dependent synergy, nor have there been avenues to exploit this information *in vivo* for combinations where ratio dependency was observed in cell culture. Historically, such correlations have been complicated by the fact that different agents in a conventional drug combination will be distributed and metabolized differentially and independently after administration, thereby precluding control of the ratio of drugs in a combination that reaches the tumor. However, drug delivery systems, such as the liposome-based carriers used here, provide a means to maintain fixed drug ratios after injection, thus providing an avenue to determine whether drug ratio dependency seen *in vitro* can be translated *in vivo*. Liposomes minimize first-pass metabolism/distribution for encapsulated drugs and preferentially accumulate at sites of tumor growth (see Fig. 4; refs. 39–41). Together, these features provide pharmacokinetic control of drug combinations previously unachievable with conventional, aqueous-based drug formulations, thereby enabling the concept of drug ratio–dependent antitumor activity to be tested directly *in vivo*.

Here, we have taken a mechanistically unbiased approach to assess the importance of drug ratios in determining the therapeutic activity of anticancer drug combinations *in vivo*. Evidence of drug ratio–dependent antitumor activity was observed for three combinations of drugs with very different mechanisms of action and clinical use. This suggests that the role of drug ratios in determining the activity of anticancer drug combinations may be of broad importance. In all cases, drug ratio–dependent synergy/antagonism relationships observed *in vitro* were consistent with *in vivo* trends in efficacy when drug ratios were maintained after injection using liposomal delivery systems. Specifically, liposomal fixed drug ratios shown to interact synergistically provided increased therapeutic activity, whereas drug ratios that yielded antagonism *in vitro* exhibited reduced efficacy

when delivered *in vivo* in liposomes. How these relationships are manifested in human cancers, where increased tumor cell heterogeneity is expected, will be revealed through extensive clinical evaluation, which is currently under way with the irinotecan/floxuridine fixed drug ratio formulation, CPX-1 (42).

Although drug combinations were not selected or evaluated on the basis of specific mechanisms, previous literature reports provide evidence that supports the ratio dependency observed here for irinotecan/floxuridine (43, 44). Specifically, examination of cell cycle checkpoint responses to floxuridine exposure in colorectal cancer cell lines has revealed that floxuridine cytotoxicity in HT-29 cells is associated with progression through S phase and drug-induced premature mitotic entry (43). At high irinotecan/floxuridine ratios (e.g., 10:1), irinotecan may antagonize floxuridine activity by arresting cells in S phase (44), which would inhibit mitotic entry. Given that irinotecan will induce DNA single-strand breaks predominantly during G_1 and S phase, it is conceivable that higher relative amounts of floxuridine (e.g., 1:1 irinotecan/floxuridine molar ratio) may drive the progression to mitosis and increase the degree of cytotoxicity in HT-29 cells by propagating deleterious DNA damage before the lesions can be repaired. This type of interaction would reflect a class 2 mechanism as defined by Rideout and Chou (28) where drug A affects cell cycle kinetics, thereby altering the biological effects of drug B after target binding. Furthermore, it is possible that this ratio dependency for simultaneous drug exposure may reflect changes in the tumor cells previously associated with sequential drug exposure where irinotecan preceding 5-fluorouracil was synergistic, whereas the reverse sequence was antagonistic (18). Whether drug ratio effects, such as those observed here for simultaneous treatment, also occur for sequential administration of drug combinations is unknown.

Based on the data presented here as well as historical evidence, we conclude that ratiometric dosing (controlling drug ratios following systemic administration) of anticancer drug combinations can profoundly influence therapeutic outcomes. We raise the possibility that currently used combination regimens, which have been developed principally by considering drug tolerabilities, may be providing less than maximum therapeutic activity. Further, by demonstrating that drug combinations can be optimized preclinically through pharmacokinetic control, we provide a new paradigm by which preclinical information can be used more directly and efficiently in clinical drug combination development. Ultimately, this should yield more effective oncology products.

References

1. Frei E III. Clinical studies of combination chemotherapy for cancer. In: Chou TC, Rideout DC, editors. Synergism and antagonism in chemotherapy. San Diego (California): Academic Press; 1991. p. 103–8.

2. DeVita VT, Jr. Principles of cancer management: chemotherapy. In: DeVita Jr, Hellman S, Rosenberg SA, editors. CANCER: principles and practice of oncology, vol. 1. Philadelphia: Lippincott-Raven; 1997. p. 333–47.

3. Tannock I. In: Tannock IF, Hill RP, editors. Basic science of oncology. New York: McGraw-Hill; 1992. p. 139–96.

4. Villalona-Calero MA, Wientjes MG, Otterson GA, et al. Phase I study of low-dose suramin as a chemosensitizer in patients with advanced non-small cell lung cancer. Clin Cancer Res 2003;9:3303–11.

5. Kerbel R, Folkman J. Clinical translation of angiogenesis inhibitors. Nat Rev Cancer 2002;2:727–39.

6. Hanahan D, Bergers G, Bergsland E. Less is more, regularly: metronomic dosing of cytotoxic drugs can target tumor angiogenesis in mice. J Clin Invest 2000;105:1045–7.

7. Teicher BA. Assays for *in vitro* and *in vivo* synergy. In: Buolamwini JK, Adjei AA, editors. Methods in molecular medicine. Novel anticancer drug protocols, vol. 85. Totowa (New Jersey): Humana Press; 2003. p. 297–321.

8. Greco WR, Bravo G, Parsons JC. The search for synergy: a critical review from a response surface perspective. Pharmacol Rev 1995;47: 331–85.

9. Tallarida RJ. Drug synergism: its detection and applications. J Pharmacol Exp Ther 2001;298:865–72.

10. Berenbaum MC. Isobolographic, algebraic, and search methods in the analysis of multiagent synergy. J Am Cell Toxicol 1998;7:927–38.

11. Tsai CM, Gazdar AF, Venzon DJ, et al. Lack of *in vitro* synergy between etoposide and *cis*-diamminedichloroplatinum(II). Cancer Res 1989;49:2390–7.

12. Gitler MS, Monks A, Sausville EA. Preclinical models for defining efficacy of drug combinations: mapping the road to the clinic. Mol Cancer Ther 2003;2:929–32.

13. Song S, Wientjes MG, Walsh C, Au JL. Non-toxic doses of suramin enhance activity of paclitaxel against lung metastases. Cancer Res 2001; 61:6145–50.

14. Kanzawa F, Koizumi F, Koh Y, et al. *In vitro* synergistic interactions between the cisplatin analogue nedaplatin and the DNA topoisomerase I inhibitor irinotecan and the mechanism of this interaction. Clin Cancer Res 2001;7:202–9.

15. Raitanen M, Rantanen V, Kulmala J, Helenius H, Grenman R, Grenman S. Supra-additive effect with concurrent paclitaxel and cisplatin in vulvar squamous cell carcinoma *in vitro*. Int J Cancer 2002;100:238–43.

16. Johnston JS, Johnson A, Gan Y, Guillaume Wientjes M, Au L-S. Synergy between 3′-azido-3′-deoxythymidine and paclitaxel in human pharynx FaDu cells. Pharm Res 2003;20:957–61.

17. Aung TT, Davis MA, Ensminger WD, Lawrence TS. Interaction between gemcitabine and mitomycin-C *in vitro*. Cancer Chemother Pharmacol 2000;45:38–42.

18. Pavillard V, Kherfellah D, Richard S, Robert J, Montaudon D. Effects of the combination of camptothecin and doxorubicin or etoposide on rat glioma cells and camptothecin-resistant variants. Br J Cancer 2001;85: 1077–83.

19. Mosmann T. Rapid colorimetric assay for cellular growth and survival: application to proliferation and cytotoxicity assays. J Immunol Methods 1983;65:55–63.

20. Chou TC, Talalay P. Quantitative analysis of dose-effect relationships: the combined effects of multiple drugs or enzyme inhibitors. Adv Enzyme Regul 1984;22:27–55.

21. Chou TC, Hayball MP. CalcuSyn: Windows software for dose effects analysis [manual]. Montana: Biosoft; 1996. p. 1–56.

22. Hope MJ, Bally MB, Webb G, Cullis PR. Production of large unilamellar vesicles by a rapid extrusion procedure: characterization of size, trapped volume and ability to maintain a membrane potential. Biochim Biophys Acta 1985;812:55–65.

23. Euhus DM, Hudd C, LaRegina MC, Johnsom FE. Tumor measurement in the nude mouse. J Surg Oncol 1986;31:229–34.

24. Tomayka MM, Reynolds CP. Determination of subcutaneous tumor size in athymic (nude) mice. Cancer Chemother Pharmacol 1989;24:148–54.

25. Skipper HE, Schabel FM, Jr., Wilcox WS. Experimental evaluation of potential anticancer agents XIII: on the criteria and kinetics associated with curability of experimental leukemia. Cancer Chemother Rep 1964;35: 1–111.

26. Skipper HE. Laboratory models: the historical perspective. Cancer Treat Rep 1986;70:3–7.

27. Waud WR. Murine L1210 and P388 leukemias. In: Teicher BA, editor. Anticancer drug development guide. Totowa (New Jersey): Humana Press; 1997. p. 59–74.

28. Rideout DC, Chou TC. Synergy, antagonism and potentiation in chemotherapy: An overview. In: Rideout DC, Chou TC, editors. Synergism and antagonism in chemotherapy. San Diego (California): Academic Press; 1991. p. 3–60.

29. Chou JH. Quantitation of synergism and antagonism of two or more drugs by computerized analysis. In: Chou TC, Rideout DC, editors. Synergism and antagonism in chemotherapy. San Diego (California): Academic Press; 1991. p. 223–41.

30. Guichard S, Cussac D, Hennebelle I, Bugat R, Canal P. Sequence-dependent activity of the irinotecan-5FU combination in human colon-cancer model HT-29 *in vitro* and *in vivo*. Int J Cancer 1997;73:729–34.

31. Pavillard V, Formento P, Rostagno P, et al. Combination of irinotecan (CPT-11) and 5-fluorouracil with an analysis of cellular determinants of drug activity. Biochem Pharmaco 1998;56:1315–22.

32. Mans DRA, Grivicich I, Peters GJ, Schwartsmann G. Sequence-dependent growth inhibition and DNA damage formation by the irinotecan-5-fluorouracil combination in human colon carcinoma cell lines. Eur J Cancer 1999;35:1851–62.

33. Ramsay E, Alnajim J, Anantha M, et al. A novel approach to prepare a liposomal irinotecan formulation that exhibits significant therapeutic activity *in vivo*. Proc Am Assoc Cancer Res 2004;45:639.

34. Cao S, Zhang Z, Creaven PJ, Rustum YM. 5-fluoro-2″-deoxyuridine: role of schedule in its therapeutic efficacy. In: Rustum YM, editor. Novel approaches to selective treatments of human solid tumors: laboratory and clinical correlation. New York: Plenum Press; 1993. p. 1–8.

35. Corbett T, Valeriote F, LoRusso P, et al. *In vivo* methods for screening and preclinical testing. In: Teicher BA, editor. Anticancer drug development guide: preclinical screening, clinical trials, and approval. Totowa (New Jersey): Humana Press; 1997. p. 75–99.

36. Frei E III, Cannellos GP. Dose a critical factor in cancer chemotherapy. Am J Med 1980;69:585–94.

37. Rowinsky EK. The pursuit of optimal outcomes in cancer therapy in a new age of rationally designed target-based anticancer agents. Drugs 2000;60:1–14.

38. Talmadge JE. Pharmacodynamic aspects of peptide administration biological response modifiers. Adv Drug Deliv Rev 1998;33:241–52.

39. Allen TM, Cullis PR. Drug delivery systems: entering the mainstream. Science 2004;303:1818–22.

40. Krishna R, McIntosh N, Riggs KW, Mayer LD. Doxorubicin encapsulated in sterically stabilized liposomes exhibits renal and biliary clearance properties that are independent of Valspodar (PSC 833) under conditions that significantly inhibit nonencapsulated drug excretion. Clin Cancer Res 1999;5:2939–47.

41. Harrington KJ, Mohammadtaghi S, Uster PS, et al. Effective targeting of solid tumors in patients with locally advanced cancers by radiolabeled pegylated liposomes. Clin Cancer Res 2001;7:243–54.

42. Batist G, Chi K, Miller W, et al. Phase 1 Study of CPX-1, a fixed ratio formulation of irinotecan (IRI) and floxuridine (FLOX), in patients with advanced solid tumors. Proc Am Soc Clin Oncol 2006;24:82.

43. Parsels LA, Parsels JD, Tai DCH, Coughlin DJ, Maybaum J. 5-Fluoro-2-deoxyuridine-induced cdc25A accumulation correlates with premature mitotic entry and clonogenic death in human colon cancer cells. Cancer Res 2004;64:6588–94.

44. Goldwasser F. Shimizu T, Jackman J, et al. Correlations between S and G_2 arrest and the cytotoxicity of camptothecin in human colon carcinoma cells. Cancer Res 1996;56:4430–7.

Molecular Cancer Therapeutics

Ratiometric dosing of anticancer drug combinations: Controlling drug ratios after systemic administration regulates therapeutic activity in tumor-bearing mice

Lawrence D. Mayer, Troy O. Harasym, Paul G. Tardi, et al.

Updated version	Access the most recent version of this article at: http://mct.aacrjournals.org/content/5/7/1854

Cited articles	This article cites 33 articles, 11 of which you can access for free at: http://mct.aacrjournals.org/content/5/7/1854.full#ref-list-1
Citing articles	This article has been cited by 12 HighWire-hosted articles. Access the articles at: http://mct.aacrjournals.org/content/5/7/1854.full#related-urls

E-mail alerts	Sign up to receive free email-alerts related to this article or journal.
Reprints and Subscriptions	To order reprints of this article or to subscribe to the journal, contact the AACR Publications Department at pubs@aacr.org.
Permissions	To request permission to re-use all or part of this article, use this link http://mct.aacrjournals.org/content/5/7/1854. Click on "Request Permissions" which will take you to the Copyright Clearance Center's (CCC) Rightslink site.